The Effects of Anion Variation and Ligand Derivatization on Silver Coordination Networks Based upon Weaker Interactions

Natalia J. Melcer,[†] Gary D. Enright,[‡] John A. Ripmeester,[‡] and George K. H. Shimizu*[,†]

Department of Chemistry, University of Calgary, 2500 University Drive N.W., Calgary, Alberta T2N 1N4, Canada, and Steacie Institute for Molecular Sciences, National Research Council of Canada, 100 Sussex Drive, Ottawa, Ontario K1A 0R6, Canada

Received April 6, 2001

This article presents a series of silver(I) coordination networks based upon nonchelating bidentate thioether ligands. Frameworks using AgOTs as the silver(I) starting material form two-dimensional frameworks and are quite stable as shown by differential scanning calorimetry/thermogravimetric analysis (DSC/TGA) data. The networks are sufficiently robust as to maintain the same layered motif when the basic skeleton of the ligand is sequentially derivatized with −OEt, OBu, and OHex groups. Crystal structures of the AgOTs complexes of the underivatized and bis(hexoxy) derivatives, compounds **5** and **8**, respectively, are presented as well as powder X-ray diffraction (PXRD) data of the other complexes. For **5**, $C_{20}H_{20}S_3O_3Ag$, crystal data are as follows: monoclinic, space group $P2_1/n$, $a = 11.8117(5)$ Å, $b = 7.8813(5)$ Å, $c = 22.3316(10)$ Å, $\beta = 102.245(5)°$, $V = 2031.6(2)$ Å^3, $Z = 4$. For **8**, $C_{30}H_{44}S_3O_6Ag$, crystal data are as follows: triclinic, space group $P\bar{1}$, $a = 8.445(4)$ Å, $b = 10.855(5)$ Å, $c = 19.308(9)$ Å, $\alpha = 84.53(1)°$, $\beta = 78.76(1)°$, $\gamma = 68.43(1)°$ $V = 1613.9(13)$ Å^3, $Z = 2$. Changing the silver(I) starting material to $AgPF_6$ results in a shift to a one-dimensional structure, **9**, as shown by X-ray crystallography and in highly compromised stability. For **9**, $C_{14}H_{16}S_2N_2PF_6Ag$, crystal data are as follows: monoclinic, space group $P2/n$, $a = 11.9658(11)$ Å, $b = 3.9056(4)$ Å, $c = 19.6400(18)$ Å, $\beta = 92.87(1)°$, $V = 916.70(15)$ Å^3, $Z = 4$.

Introduction

Fundamental to directing the properties of a given network solid is the ability to regulate its structure. In this regard, coordination frameworks have great potential owing to their threefold tunability.[1] The first two adjustable variables are the structural diversity resulting from the choice of cation and anion. The third factor is the variation of the organic ligand. Typically, this is accomplished by altering the structure of the linker unit, varying the nature of the coordinating atom, or both. A distinct advantage of coordination networks over solely inorganic frameworks is the prospect of organic derivatization of the ligands. Unfortunately, as often is the case, small adaptations in ligand structure can produce greater alterations to the complex than had been desired, yielding new frameworks rather than modified parent networks.[2,3] With regards to the donor atom in studies of coordination frameworks, thioether donors have been studied to a relatively small extent.[4] This owes to the observation that monodentate thioethers are generally poor ligands and thus would be unfavorable for the generation of robust solids.[5] The present article presents a family of Ag thioether networks which illustrate that such individually weak metal−ligand interactions

* To whom correspondence should be addressed. Tel: (403) 220-5347. Fax: (403) 289-9488. E-mail: gshimizu@ucalgary.ca.

† University of Calgary.

‡ National Research Council of Canada.

(1) For recent reviews, see: (a) Batten, S. R.; Robson, R. *Angew. Chem.* **1998**, *110*, 1558; *Angew. Chem., Int. Ed.* **1998**, *37*, 1460. (b) Blake, A. J.; Champness, N. R.; Hubberstey, P.; Li, W.-S.; Withersby, M. A.; Schröder, M. *Coord. Chem. Rev.* **1999**, *183*, 117. (c) Bowes, C. L.; Ozin, G. A. *Adv. Mater.* **1996**, *8*, 13. (d) Munakata, M.; Wu, L. P.; Kuroda-Sowa, T. *Bull. Chem. Soc. Jpn*. **1997**, *70*, 1727. (e) Yaghi, O. M.; Li, H.; Davis, C.; Richardson, D.; Groy, T. L. *Acc. Chem. Res.* **1998**, *31*, 474. For recent leading articles, see: (f) Seo, J. S.; Whang, D.; Lee, H.; Jun, S. I.; Oh, J.; Jeon, Y. J.; Kim, K. *Nature* **2000**, *404*, 982. (g) Li, H.; Eddaoudi, M.; O'Keeffe, M.; Yaghi, O. M. *Nature* **1999**, *402*, 276. (h) Chui, S. S.-Y.; Lo, S. M.-F.; Charmant, J. P. H.; Orpen, A. G.; Williams, I. D. *Science* **1999**, *283*, 1148. (i) Goodgame, D. M. L.; Grachvogel, D. A.; Williams, D. J. *Angew. Chem.* **1999**, *111*, 217; *Angew. Chem., Int. Ed.* **1999**, *38*, 153. (j) Eddaoudi, M.; Li, H.; Yaghi, O. M. *Angew. Chem., Int. Ed.* **2000**, *122*, 1391. (k) Biradha, K.; Aoyagi, M.; Fujita, M. *Angew. Chem., Int. Ed.* **2000**, *122*, 2397. (l) Kepert, C. J.; Prior, T. J.; Rosseinsky, M. J. *Angew. Chem., Int. Ed.* **2000**, *122*, 2397.

(2) (a) Bishop, R.; Choudry, S.; Dance, I. *J. Chem. Soc., Perkin Trans. 2* **1982**, 1159. (b) Fujita, M.; Kwon, Y.; Sasaki, O.; Yamaguchi, K.; Ogura, K. *J. Am. Chem. Soc*. **1995**, *117*, 7.

(3) The work of Lee et al. on tunable channel structures is a fine example of an exception to this previous statement. Kiang, Y.-H.; Gardner, G. B.; Lee, S.; Xu, Z.; Lobkovsky, E. B. *J. Am. Chem. Soc*. **1999**, *121*, 8204.

(4) (a) Suenaga, Y.; Kuroda-Sowa, T.; Munakata, M.; Maekawa, M.; Morimoto, H. *Polyhedron* **1999**, *18*, 429. (b) Suenaga, Y.; Maekawa, M.; Kuroda-Sowa, T.; Munakata, M.; Morimoto, H.; Hiyama, N.; Kitagawa, S. *Anal. Sci.* **1997**, *13*, 1047. (c) Yamamoto, M.; Wu, L. P.; Kuroda-Sowa, T.; Maekawa, M.; Suenaga, Y.; Munakata, M. *Inorg. Chim. Acta* **1997**, *258*, 87. (d) Barton, A. J.; Hill, N. J.; Levason, W.; Patel, B.; Reid, G. *Chem. Commun*. **2001**, 95. (e) Black, J. R.; Champness, N. R.; Levason, W.; Reid, G. *Inorg. Chem.* **1996**, *35*, 1820. (f) Barton, A. J.; Genge, A. R. J.; Levason, W.; Reid, G. *J. Chem. Soc., Dalton Trans*. **2000**, 859. (g) Blake, A. J.; Champness, N. R.; Howdle, S. M.; Webb, P. B. *Inorg. Chem*. **2000**, *39*, 1035. (h) Blake, A. J.; Li, W.-S.; Lippolis, V.; Schröder, M. *Chem. Commun.* **1997**, 1943. (i) Alberto, R.; Angst, D.; Abram, U.; Ortner, K.; Kaden, T. A.; Schubiger, A. P. *Chem. Commun*. **1999**, 1513. (j) Blake, A. J.; Gould, R. O.; Li, W.-S.; Lippolis, V.; Parsons, S.; Radek, C.; Schröder, M. *Inorg. Chem*. **1998**, *37*, 5070. (k) Munakata, M.; Wu, L. P.; Yamamoto, M.; Kurodo-Sowa, T.; Maekawa, M. *J. Chem. Soc., Dalton Trans.* **1995**, 3215. (l) Blake, A. J.; Collison, D.; Gould, R. O.; Reid, G.; Schröder, M. *J. Chem. Soc., Dalton Trans.* **1993**, 521. (m) Buter, J.; Kellogg, R. M.; van Bolhuis, F. *J. Chem. Soc., Chem. Commun*. **1991**, 910. (n) Suenaga, Y.; Kuroda-Sowa, T.; Maekawa, M.; Munakata, M. *J. Chem. Soc., Dalton Trans.* **1999**, 2737.

(5) Cooper, S. R. *Acc. Chem. Res*. **1988**, *21*, 141.

10.1021/ic0103749 CCC: $20.00
Published on Web 07/26/2001

can still yield robust networks through cooperative bonding effects. Indeed, these frameworks adopt similar structural motifs even when the thioether ligand is derivatized. An illustration is also made of how the stability of frameworks is compromised when the dimensionality of the extended structure is reduced via changing the counteranion of the framework.

In our prior work, we have shown that the dithia ligand, **1**, forms infinite two-dimensional (2-D) networks with $AgBF_4$.[6] In addition to possessing cationic layers, these networks demonstrated solvent-dependent swelling, leading to an analogy to anionic clays.[7,8] Herein, the previous work is extended by illustrating the effects of anion variation as well as ligand modification in the Ag(**1**)$^+$ family. We present a systematically derivatized series of ligands, **1**−**4**, and their AgOTs complexes,

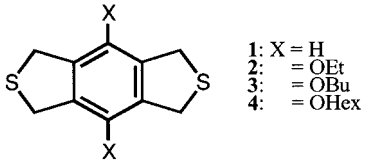

1: X = H
2: = OEt
3: = OBu
4: = OHex

5−**8**,[9] respectively, as well as the complex Ag(**1**)PF_6, **9**. Complexes **5**−**8** all form layered or "decorated" layered structures and are quite stable. Changing to the PF_6^- ion in complex **9** results in a shift to a one-dimensional (1-D) structure as shown by X-ray crystallography and as evidenced by the compromised stability of **9**.

Experimental Section

Materials and Methods. NMR spectra were obtained using a Bruker ACT 200 MHz spectrometer using $CDCl_3$ as the solvent. Powder X-ray diffraction (PXRD) data were collected on a Scintag SDX2000 powder diffractometer in the Geology and Geophysics Department at the University of Calgary. Mass spectral data were acquired using a VG77 mass spectrometer. Elemental analyses were performed at the University of Calgary. All experiments were performed, unless otherwise stated, under an anhydrous nitrogen atmosphere. Solvents were dried appropriately and distilled under nitrogen. Ligand **1** was prepared as reported previously.[6] The bis(alkoxy)derivative precursors to **2**−**4** were prepared in three steps from duroquinone as reported by Müllen et al.[10]

Synthesis of 2. The bis(ethoxy)tetrabromodurene derivative (2.19 g, 4.1 mmol) was dissolved in ethanol (200 mL). Sodium sulfide nonahydrate (2.15 g, 9.0 mmol) was then added, and the solution was refluxed with stirring for 12 h. It was then cooled to room temperature, vacuum filtered, and concentrated in vacuo. The resulting off-white residue as well as the originally filtered solid was extracted with ethyl acetate. The combined extracts were washed gently with water (3 × 30 mL), dried over sodium sulfate, filtered, and concentrated in vacuo to afford the product (0.92 g, 3.3 mmol, 80%) as an off-white powder. (Note: in the ^{1}H NMR, two conformers of the ether groups (cis and trans to the face of the benzene) are apparent.) ^{1}H NMR δ: 4.21 (s, 8H, Ar−CH_2−S−), 4.12 (q, J = 7 Hz, 4H, −OCH_2− (cis or trans)), 3.93 (q, J = 7 Hz, 4H, −OCH_2− (cis or trans)), 1.36 (t, J = 7 Hz, 6H, −CH_3 (cis or trans)), 1.26 (t, J = 7 Hz, 6H, −CH_3 (cis or trans)). ^{13}C{^{1}H} NMR: δ 146.91 (−**C**(OEt)), 134.58 (−**C**(CH_2−S−)), 68.34 (−CH_2−S−), 35.08 (−OCH_2−), 15.97 (−CH_3). MS *m*/*e*: 282 (M^+), 253 (M^+ − Et). Anal. Calcd for $C_{14}H_{18}O_2S_2$: C, 59.54; H, 6.42. Found: C, 58.87; H, 6.25.

Synthesis of 3 and 4. These were prepared analogously to **2**, beginning with the appropriate bis(alkoxy)tetrabromodurene derivative. For **3**, yield was 79% as an off-white solid. ^{1}H NMR: δ 4.22 (s, 8H, Ar−CH_2−S−), 3.85 (t, J = 6.5 Hz, 4H, −OCH_2−), 1.72 (m, 4H, −$OCH_2C\mathbf{H_2}$−), 1.49 (m, 4H, −$C\mathbf{H_2}CH_3$), 0.98 (t, J = 7.3 Hz, 6H, −CH_3). ^{13}C{^{1}H} NMR δ: 147.06 (−**C**(OBu)), 134.51 (−**C**(CH_2−S−)), 72.57 (−CH_2−S−), 35.08 (−OCH_2−), 32.55 (−$OCH_2\mathbf{C}H_2$−), 19.29 (−$\mathbf{C}H_2CH_3$), 13.92 (−CH_3). MS *m*/*e*: 338 (M^+), 282 (M^+ − Bu), 226 (M^+ − 2Bu). Anal. Calcd for $C_{18}H_{26}O_2S_2$: C, 63.86; H, 7.74. Found: C, 63.18; H, 7.30. For **4**, yield was 75% as an off-white solid. ^{1}H NMR: δ 4.22 (s, 8H, Ar−CH_2−S−), 3.84 (t, J = 6.5 Hz, 4H, −OCH_2−), 1.74 (m, 4H, −$OCH_2C\mathbf{H_2}$−), 1.60−1.25 (m, 12H, −$C\mathbf{H_2}C\mathbf{H_2}C\mathbf{H_2}$-$CH_3$), 0.91 (t, J = 7.3 Hz, 6H, −CH_3). ^{13}C{^{1}H} NMR δ: 146.99 (−**C**(OHex)), 134.44 (−**C**(CH_2−S−)), 72.82 (−CH_2−S−), 35.03 (C1), 31.60 (C2), 30.39 (C3), 25.67 (C4), 22.56 (C5),14.00 (C6). MS *m*/*e*: 394 (M^+), 310 (M^+ − Hex), 226 (M^+ − 2Hex). Anal. Calcd for $C_{22}H_{34}O_2S_2$: C, 66.96; H, 8.68. Found: C, 66.49; H, 8.55.

General Preparation of Ag Complexes. In a typical preparation, 1.00 mmol of the appropriate Ag starting material was added to a degassed MeCN solution (20 mL) of the appropriate ligand, **1**−**4** (1.00 mmol), and the flask was wrapped in aluminum foil. The solution was again degassed and stirred for 12 h at room temperature under N_2. Diethyl ether (10 mL) was added to precipitate product. The off-white products were filtered and dried in vacuo. Elemental analysis confirmed a 1:1 stoichiometry of metal/ligand for each of **5**−**8**. Complex **9** was studied as single-crystal material: [Ag(**1**)OTs], **5**; [Ag(**2**)OTs], **6**; [Ag(**3**)OTs], **7**; [Ag(**4**)OTs], **8**; [Ag(**1**)(MeCN)]PF_6, **9**. For **5**, yield: 98%. Anal. Calcd for $C_{17}H_{17}AgO_3S_3$: C, 43.13; H, 3.62. Found: C, 43.08; H, 3.59. For **6**, yield: 96%. Anal. Calcd for $C_{21}H_{25}AgO_5S_3$: C, 44.92; H, 4.49. Found: C, 44.85; H, 4.44. For **7**, yield: 91%. Anal. Calcd for $C_{25}H_{33}AgO_5S_3$: C, 48.62; H, 5.39. Found: C, 48.55; H, 5.33. For **8**, yield: 83%. Anal. Calcd for $C_{29}H_{41}AgO_5S_3$: C, 51.70; H, 6.13. Found: C, 51.62; H, 6.08. For **9**, yield 39%. Anal. Calcd for $C_{12}H_{13}AgF_6NPS_2$: C, 29.52; H, 2.68. Found: C, 27.77; H, 2.20.

General X-ray Crystallography. Crystals were selected under an optical microscope, coated in oil, and frozen onto a glass fiber. Data were collected on a Siemens SMART CCD diffractometer (Mo Kα radiation, λ = 0.710 73 Å) using the ω scan mode (3° < 2θ < 57.3°). Structures were solved by direct methods and refined by full-matrix least-squares, based on F^2, using the NRCVAX suite of programs[11] for compound **5** and SHELXTL[12] for compounds **8** and **9**. Silver and sulfur atoms were located first, and the remaining atoms were found by difference Fourier maps. All non-hydrogen atoms were refined anisotropically.

Single-Crystal Structure Determination of 5·(Benzene)$_{0.5}$. A colorless platelike crystal of dimensions 0.04 × 0.20 × 0.20 mm^3 was employed. The lattice parameters are as follows: a = 11.8817(5) Å, b = 7.8813(5) Å, c = 22.332(1) Å, β = 102.245(5)°, V = 2031.6(2) Å^3, space group is $P2_1/n$, and Z = 4. A total of 22 941 reflections were measured, and these were merged to give 5244 unique reflections (R_{merg} = 0.029), 4175 of which were considered to be observed when I > 2.5σ(I). A summary of pertinent crystal data is presented in Table 1. Final R values for significant data (R = 2.9%, R_w = 5.3%, GOF = 1.92) were obtained for a total of 324 parameters. In the last D-map, the deepest hole was −0.400 e/Å^3 and the highest peak was 0.530 e/Å^3. Fractional atomic coordinates are given in Table 2, and selected bond distances and angles are given in Table 3.

Single-Crystal Structure Determination of 8·MeOH. A colorless platelike crystal of dimensions 0.32 × 0.08 × 0.03 mm^3 was employed. The lattice parameters are as follows: a = 8.445(4) Å, b = 10.855(5) Å, c = 19.308(9) Å, α = 84.53(1)°, β = 78.66(1)°, γ = 68.43(1)°, V = 1613.9(13) Å^3, space group is $P\bar{1}$, and Z = 2. A total of 14 191

(6) Shimizu, G. K. H.; Enright, G. D.; Ratcliffe, C. I.; Ripmeester, J. A.; Wayner, D. D. M. *Angew. Chem.* **1998**, *110*, 1510; *Angew. Chem., Int. Ed.* **1998**, *37*, 1407.
(7) (a) Occelli, M. A.; Robson, H. *Expanded Clays and Other Microporous Solids*; Academic Press: New York, 1992. (b) Mitchell, I. V. *Pillared Layered Structures*; Elsevier Applied Science: New York, 1990.
(8) For other clay mimics, see: (a) Biradha, K.; Dennis, D.; MacKinnon, V. A.; Sharma, C. V. K.; Zaworotko, M. J. *J. Am. Chem. Soc.* **1998**, *120*, 11894. (b) Coleman, A. W.; Bott, S. G.; Morley, S. D.; Means, C. M.; Robinson, K. D.; Zhang, H.; Atwood, J. L. *Angew. Chem.* **1988**, *100*, 1412; *Angew. Chem., Int. Ed.* **1988**, *27*, 1361.
(9) Compound **5** has been the subject of a preliminary communication. Shimizu, G. K. H.; Enright, G. D.; Ratcliffe, C. I.; Ripmeester, J. A. *Chem. Commun*. **1999**, 461.
(10) Röhrich, J.; Müllen, K. *J. Org. Chem*. **1992**, *57*, 2374.
(11) Gabe, E. J.; Charland, J.-P.; Lee, F. L.; White, P. S. *J. Appl. Crystallogr*. **1989**, *22*, 384.
(12) *SHELXTL*, version 5.1; Bruker AXS Inc.: Madison, Wisconsin, 1997.

Table 1. Crystal Data and Refinement Summaries for Compounds **5**, **8**, and **9**

formula	$C_{20}H_{20}S_3O_3Ag$, **5**·$(C_6H_6)_{0.5}$	$C_{30}H_{44}S_3O_6A_g$, **8**·MeOH	$C_{14}H_{16}S_2N_2PF_6Ag$, **9**
fw	512.42	704.71	529.24
cryst syst	monoclinic	triclinic	monoclinic
space group	$P2_1/n$ (No. 14)	$P\bar{1}$ (No. 2)	$P2/n$ (No. 13)
a (Å)	11.8117(5)	8.445(4)	11.966(1)
b (Å)	7.8813(5)	10.855(5)	3.9056(4)
c (Å)	22.332(1)	19.308(9)	19.640(2)
α (deg)		84.53(1)	
β (deg)	102.245(5)	78.76(1)	92.87
γ (deg)		68.43(1)	
V (Å^3)	2031.6(2)	1614(1)	916.7(1)
T (°C)	−100	−100	−100
Z	4	2	4
D_{calcd} (g/cm^3)	1.675	1.452	1.917
μ (mm^{-1})	1.32	0.858	1.473
radiation, λ (Å)	0.709 30	0.709 30	0.709 30
R_f (sig reflns)[a]	0.029	0.076	0.053
R_w (sig reflns)[b]	0.028	0.1589	0.111

[a] $R_f = (\sum(F_o - F_c)/\sum(F_o)$. [b] $R_w = (\sum w(F_o - F_c)^2/\sum w(F_o)^2)^{0.5}$.

Table 2. Atomic Parameters for Non-Hydrogen Atoms of Compound **5**

	x	*y*	*z*	*biso*
Ag	0.264 989(19)	0.706 76(3)	0.199 189(8)	2.337(8)
S1	0.207 38(6)	0.825 38(8)	0.091 52(3)	1.90(3)
S2	−0.173 23(6)	0.589 88(8)	−0.209 54(3)	1.783(24)
S3	0.474 78(6)	0.426 38(8)	0.259 25(3)	1.907(24)
O1	0.418 64(18)	0.4811(3)	0.307 97(9)	3.90(11)
O2	0.441 58(19)	0.257 70(25)	0.237 53(12)	4.38(11)
O3	0.460 00(16)	0.551 30(24)	0.210 55(8)	2.72(8)
C1	0.049 74(23)	0.8049(3)	0.069 73(10)	1.90(10)
C2	0.026 46(22)	0.7441(3)	0.004 57(10)	1.50(9)
C3	0.121 63(22)	0.6766(3)	−0.014 87(10)	1.60(9)
C4	0.232 56(23)	0.6753(3)	0.033 51(11)	2.03(10)
C5	−0.081 30(23)	0.7517(3)	−0.035 54(11)	1.70(10)
C6	−0.091 71(21)	0.6947(3)	−0.095 61(10)	1.62(9)
C7	0.003 47(22)	0.6286(3)	−0.114 83(10)	1.60(9)
C8	0.111 03(22)	0.6171(3)	−0.074 34(11)	1.70(10)
C9	−0.201 80(23)	0.7106(3)	−0.144 04(11)	1.99(10)
C10	−0.016 11(22)	0.5835(3)	−0.181 87(11)	1.96(10)
C11	0.625 12(22)	0.4208(3)	0.292 61(11)	1.81(10)
C12	0.699 52(25)	0.3188(3)	0.268 01(12)	2.50(12)
C13	0.817 59(25)	0.3213(3)	0.293 31(13)	2.62(12)
C14	0.863 89(23)	0.4258(3)	0.342 12(12)	2.36(11)
C15	0.787 93(24)	0.5235(3)	0.367 37(12)	2.54(11)
C16	0.669 26(23)	0.5201(3)	0.343 14(12)	2.23(11)
C17	0.9933(3)	0.4339(4)	0.366 32(15)	3.60(15)
C18	0.5516(4)	0.5360(6)	0.058 46(21)	7.6(3)
C19	0.5682(4)	0.6381(6)	0.0125(3)	9.3(3)
C20	0.5136(5)	0.5989(6)	−0.047 92(24)	8.4(3)

reflections were measured, and these were merged to give 4653 unique reflections (R_{merg} = 0.1950), 2290 of which were considered to be observed when $I > 2.0\sigma(I)$. A summary of pertinent crystal data is presented in Table 1. Final R values for significant data (R = 7.60%, R_w = 15.9%, GOF = 0.986) were obtained for a total of 343 parameters. In the last D-map, the deepest hole was −0.854 e/Å^3 and the highest peak was 1.68 e/Å^3 which was closely associated with the Ag center. The benzene core of **4** was modeled as a rigid group after generating the symmetry-related equivalents of C1, C2, C3 and C12, C13, C14 as nonrefining atoms. The benzylic carbon atom, C16, was constrained using the SIMU command. These options were necessary as the layered crystals encountered in these studies sometimes proved difficult for X-ray diffraction studies. Compound **8** was an example of this. The rocking curve was large (>1.5° ω) leading to peak overlap in certain directions. This is reflected in the poor merging R's but can be somewhat accounted for with high data redundancy (unfortunately this was not possible in a triclinic cell as in **8**). In addition, the data set for **8** was weak (less than 50% observed). The resultant data set will have somewhat greater inaccuracies in peak intensities for directions where overlap is significant (or where anisotropic extinction is important). This is expected to lead to problems such as that seen with poor absorption correction and bad thermal parameters for some atoms. Fractional atomic coordinates are given in Table 4, and selected bond distances and angles are given in Table 5.

Table 3. Selected Bond Distances and Angles for Compound **5**[a]

bond	length (Å)	bond	length (Å)
Ag−S1	2.5347(6)	Ag−S2a	2.6077(7)
Ag−S2b	2.5739(6)	Ag−O3	2.574(2)
S1−C1	1.829(3)	S1−C4	1.824(3)
S3−O1	1.455(2)	S3−O2	1.441(2)
S3−O3	1.450(2)	S3−C11	1.775(3)
bond	**angle (deg)**	**bond**	**angle (deg)**
S1−Ag−S2a	112.44(2)	S1−Ag−S2b	119.71(2)
S1−Ag−O3	108.89(4)	S2a−Ag−S2b	122.78(2)
S2a−Ag−O3	86.82(4)	S2b−Ag−O3	96.94(5)
Ag−S1−C1	105.85(8)	Ag−S1−C4	112.52(8)
Aga−S2−Agc	125.11(2)	Aga−S2−C9	104.12(9)
Aga−S2−C10	110.90(8)	Agc−S2−C9	103.84(8)
Agc−S2−C10	112.44(8)	Ag−O3−S3	111.1(1)
C1−S1−C4	93.7(1)	C9−S2−C10	95.2(1)

[a] The equivalent positions are (1) x, y, z and (2) $^1/_2 - x$, $^1/_2 + y$, $^1/_2 - z$. The lattice is primitive. There are no centering vectors.

Single-Crystal Structure Determination of 9. A colorless platelike crystal of dimensions 0.20 × 0.15 × 0.03 mm^3 was employed. The lattice parameters are as follows: a = 11.966(1) Å, b = 3.9056(4) Å, c = 19.640(2) Å, β = 92.870(5)°, V = 916.7(2) Å^3, space group is $P2/n$, and Z = 4. A total of 9857 reflections were measured, and these were merged to give 2347 unique reflections (R_{merg} = 0.0689), 1892 of which were considered to be observed when $I > 4.0\sigma(I)$. A summary of pertinent crystal data is presented in Table 1. Final R values for significant data (R = 5.30%, R_w = 11.1%, GOF = 1.062) were obtained for a total of 190 parameters. In the last D-map, the deepest hole was −0.713 e/Å^3 and the highest peak was 1.934 e/Å^3 which was, again, closely associated with the Ag center. The PF_6 ion and the coordinated MeCN molecule are disordered as described later on. Fractional atomic coordinates are given in Table 6, and selected bond distances and angles are given in Table 7.

Results and Discussion

Synthesis of Ligands and Ag Complexes. Ligand **1** was prepared as reported previously.[5] Ligands **2**−**4** were synthesized in very good yields in four steps from duroquinone. The procedure of Müllen was used to synthesize the tetrakis(bromomethyl)bis(alkoxy)benzene derivatives.[10] These compounds were subsequently reacted with 2 equiv of $Na_2S{\cdot}9H_2O$ to close the five-membered hydrothiophene rings. Stirring ligands **1**−**4** individually with AgOTs in MeCN solution, followed by solvent removal, gave the complexes Ag(**1**)OTs (**5**), Ag(**2**)OTs (**6**), Ag(**3**)OTs (**7**), and Ag(**4**)OTs (**8**) as off-white powders which were stable to both air and light. Complex **9**, [Ag(**1**)(MeCN)]PF_6, was highly air and light sensitive and required storage under N_2 in the dark.

Structures of 5·(Benzene)$_{0.5}$, 8·MeOH, and 9. For **5**, AgOTs in MeCN was added to a MeCN solution of **1** in a 1:1 molar ratio. Diffusion of benzene into this solution gave colorless, platelike crystals of {Ag(**1**)OTs·benzene$_{0.5}$}$_\infty$, **5**·(benzene)$_{0.5}$, suitable for an X-ray analysis. The structure of **5**·(benzene)$_{0.5}$ (Figure 1) reveals the formation of an infinite two-dimensional array consisting of cationic Ag(**1**) layers reinforced by a coordinating *p*-toluenesulfonate anion. The geometry at the metal center is a slightly distorted tetrahedron comprised of three thioether donors and a sulfonate oxygen (Ag−S1 = 2.5347(6)

Table 4. Atomic Parameters for Non-Hydrogen Atoms of Compound **8**

	x	*y*	*z*	*biso*
Ag	0.752 41(21)	0.498 25(16)	0.481 94(8)	2.63(7)
S1	1.0492(5)	0.3325(4)	0.466 51(21)	2.0(3)
S2	0.4524(5)	0.6698(4)	0.514 46(21)	2.0(3)
S3	0.8149(7)	0.5254(5)	0.307 04(25)	3.6(3)
O1	1.0395(13)	0.0023(10)	0.6386(5)	2.6(6)
O2	0.4509(12)	1.0279(9)	0.3614(5)	1.8(6)
O3	0.6922(16)	0.4588(11)	0.3237(6)	5.9(8)
O4	0.9853(13)	0.4355(10)	0.2921(5)	5.1(7)
O5	0.7966(13)	0.6166(11)	0.3603(5)	3.8(7)
O6	0.6577(16)	0.4291(11)	0.6245(6)	4.6(8)
C1	1.0656(18)	0.2203(14)	0.5448(7)	1.9(3)
C2	1.0312(17)	0.1027(13)	0.5236(7)	0.6(3)
C3	1.0175(17)	0.1012(13)	0.4549(7)	1.0(3)
C4	1.0434(19)	0.2112(14)	0.4085(7)	2.5(3)
C5	1.0132(18)	0.0030(14)	0.5687(8)	1.3(3)
C6	0.4276(16)	0.7959(12)	0.4440(6)	1.0(3)
C7	0.4641(16)	0.9059(12)	0.4704(7)	0.5(3)
C8	0.4816(17)	0.8921(13)	0.5398(7)	0.7(3)
C9	0.4561(17)	0.7717(13)	0.5794(6)	1.4(3)
C10	0.4816(17)	1.0117(14)	0.4303(8)	1.1(3)
C11	0.8811(20)	0.0602(15)	0.6870(8)	2.5(10)
C12	0.9178(22)	0.0227(19)	0.7609(8)	4.1(11)
C13	0.9914(22)	−0.1209(19)	0.7767(9)	4.1(11)
C14	1.023(3)	−0.1551(20)	0.8513(10)	5.3(13)
C15	1.101(3)	−0.304(3)	0.8610(9)	8.4(19)
C16	1.135(3)	−0.3526(20)	0.9340(10)	7.3(14)
C17	0.6034(21)	0.9858(14)	0.3093(8)	2.2(10)
C18	0.5574(22)	1.0362(17)	0.2376(8)	3.5(10)
C19	0.4798(20)	1.1844(17)	0.2306(8)	3.5(10)
C20	0.4423(24)	1.2292(21)	0.1564(10)	5.6(13)
C21	0.369(3)	1.3826(22)	0.1495(9)	6.0(14)
C22	0.325(3)	1.4322(20)	0.0766(10)	8.1(15)
C23	0.768(3)	0.6191(16)	0.2290(9)	3.8(11)
C24	0.615(3)	0.6491(19)	0.2085(11)	5.5(13)
C25	0.577(3)	0.7239(23)	0.1485(15)	7.0(16)
C26	0.698(4)	0.7752(23)	0.1111(11)	7.3(18)
C27	0.857(3)	0.7456(23)	0.1311(13)	6.9(15)
C28	0.887(3)	0.6692(19)	0.1916(11)	5.2(13)
C29	0.649(3)	0.8711(20)	0.0453(10)	11.9(20)
C30	0.735(3)	0.4623(16)	0.6707(10)	4.8(13)

Table 5. Selected Bond Distances and Angles for Compound **8**[a]

bond	length (Å)	bond	length (Å)
Ag−S1	2.470(4)	Ag−S2	2.532(4)
Ag−S2a	2.928(5)	Ag−S1a	3.230(5)
Ag−O5	2.596(5)	Ag−O	2.814(5)
S1−C1	1.843(14)	S1−C4	1.827(15)
S2−C6	1.820(13)	S2−C9	1.762(13)
S3−O3	1.440(14)	S3−O4	1.402(11)
S3−O5	1.443(12)	S3−C23	1.763(18)

bond	angle (deg)	bond	angle (deg)
S1−Ag−S2	172.43(15)	S1−Ag−S2a	101.46(14)
S2−Ag−S2a	80.68(13)	Ag−S2−Aga	99.32(14)
Ag−S2−C6	106.3(4)	Ag−S2−C9	108.7(5)
Ag−S1−C1	107.6(4)	Ag−S1−C4	103.9(5)
Aga−S2−C6	115.1(4)	Aga−S2−C9	130.4(5)
C1−S1−C4	94.2(6)	C6−S2−C9	95.5(6)
O3−S3−O4	111.8(7)	O3−S3−O5	113.2(7)
O4−S3−O5	111.2(7)	O3−S3−C23	105.5(9)
O4−S3−C23	107.3(8)	O5−S3−C23	107.4(7)

[a] The equivalent positions are (1) *x*, *y*, *z* and (2) −*x*, −*y*, −*z*. The lattice is primitive. There are no centering vectors.

Å, Ag−S2a = 2.6077(7) Å, Ag−S2b = 2.5739(6) Å, Ag−O3 = 2.574(2) Å). Each molecule of **1** is asymmetrically ligated to three different silver ions (Figure 2). That is, the sulfur donor

Table 6. Atomic Parameters for Non-Hydrogen Atoms of Compound **9**

	x	*y*	*z*	*biso*
Ag	2500	8726(1)	2500	30(1)
S1	1499(1)	5645(2)	1491(1)	24(1)
C1	996(3)	10 018(11)	−350(2)	20(1)
C2	974(3)	8780(10)	314(2)	21(1)
C3	2(3)	8760(10)	661(2)	19(1)
C4	91(4)	7377(11)	1373(2)	23(1)
C5	1997(4)	7418(11)	703(2)	23(1)
C6	4406(8)	12 790(20)	1523(5)	33(2)
C7	5029(11)	14 320(30)	983(6)	50(3)
C8	4915(9)	12 660(20)	1999(5)	35(2)
C9	6030(10)	14 060(40)	1973(7)	53(3)
N	3961(4)	11 574(12)	1988(2)	45(1)
P1	5000	15 000	0	39(1)
P2	7500	14 217(13)	2500	53(1)
F1	4609(6)	16 210(20)	716(3)	56(2)
F2	4008(7)	12 430(20)	−71(6)	86(3)
F3	5789(7)	12 140(20)	328(4)	70(2)
F4	7553(15)	11 520(30)	1911(7)	149(6)
F5	6234(8)	14 240(50)	2429(6)	162(8)
F6	7549(11)	16 930(30)	1920(7)	121(4)

Table 7. Selected Bond Distances and Angles for Compound **9**[a]

bond	length (Å)	bond	length (Å)
Ag−N	2.340(5)	Ag−S1	2.563(1)
S1−C4	1.819(4)	S1−C5	1.823(4)
C6−N	1.181(11)	C8−N	1.218(11)
P1−F1	1.577(6)	P1−F2	1.555(8)
P11−F3	1.580(7)	P2−F4	1.567(12)
P2−F5	1.514(10)	P2−F6	1.559(11)

bond	angle (deg)	bond	angle (deg)
N−Ag−N#1	123.2(2)	N−Ag−S1	102.79(12)
N#1−Ag−S1	103.00(13)	N−Ag−S1#1	103.00(13)
S1−Ag−S1#1	124.00(5)	C4−S1−C5	95.15(18)
C4−S1−Ag	108.56(13)	C5−S1−Ag	108.54(14)
C8−N−Ag	151.4(6)	C6−N−Ag	154.1(6)
C2−C5−S1	105.9(3)	C3−C4−S1	106.0(3)
N−C6−C7	175.8(10)	N−C8−C9	176.4(10)

[a] The equivalent positions are (1) $-x+{}^1/_2$, *y*, $-z+{}^1/_2$, (2) −*x*, −*y* + 2, −*z*, (3) −*x* + 1, −*y* + 3, −*z*, and (4) $-x+{}^3/_2$, *y*, $-z+{}^1/_2$. The lattice is primitive. There are no centering vectors.

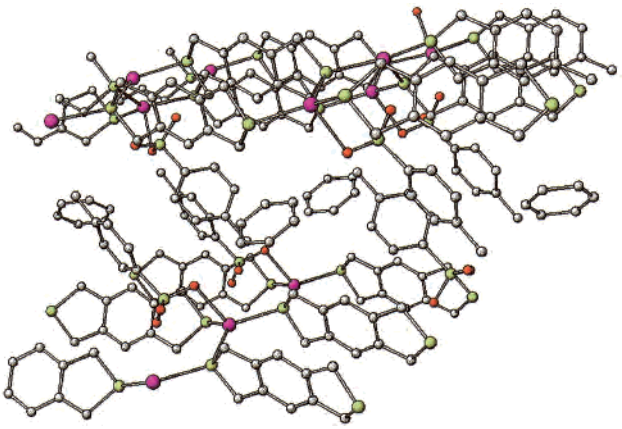

Figure 1. View of the lamellar network formed by complex **5**, showing the "pillaring" effect of the OTs anions and the inclusion of benzene in the resultant void space: Ag, large spheres; S, medium spheres; O, small dark spheres; C, small white spheres.

on one side of the ligand coordinates to two silver ions while the sulfur atom on the other side of the ligand bonds to only one, consistent with the Ag(**1**)BF_4 complexes.[6] However, in contrast to the BF_4^- complex, the Ag(**1**) network in **5**·

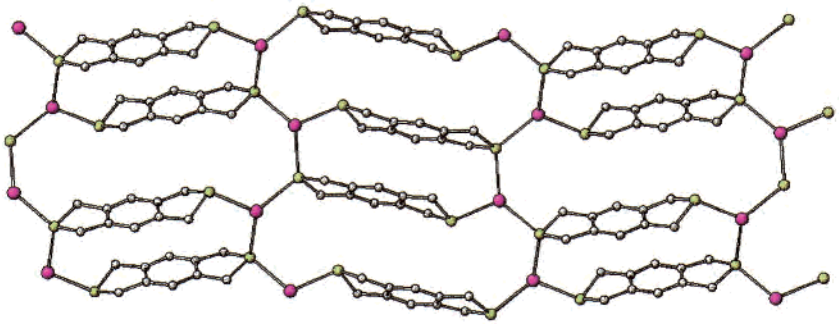

Figure 2. View of the corrugated structure of the cationic Ag(**1**) layers of **5** and the tetrahedral geometry at Ag^{I}. Note the unsymmetrical mode of coordination of **1**.

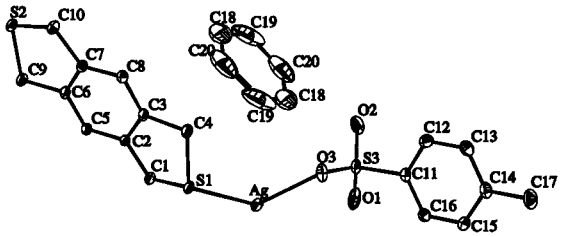

Figure 3. ORTEP plot of the asymmetric unit of **5** showing the numbering scheme. Thermal ellipsoids of 50% probability are represented.

$(benzene)_{0.5}$ does not form perfectly flat layers. In **5**·$(benzene)_{0.5}$, a corrugated motif is adopted (Figure 2), as necessitated by the tetrahedral geometry at the Ag^{I} center. The dihedral angle formed by the central benzene rings of adjacent molecules of **1** is 48.50(9)°. In **5**·$(benzene)_{0.5}$, ligand **1** is observed solely in the anti conformation, with respect to the orientation of the sulfur donors in the slightly puckered pentagonal rings. The toluenesulfonate anion is coordinated to the silver ions and orients itself at an angle of 24.2(1)° to the mean lamellar plane. The interlayer distance in **5**·$(benzene)_{0.5}$ is 11.230(1) Å (cf. 10.085(1) Å in the BF_4 salt),[6] defined as the perpendicular distance between Ag^{I} ions. Thus, the anion serves as a pillar to prop the lamellae apart and allow for inclusion of 0.5 molecules of benzene per asymmetric unit. The ligand−ligand separation, measured perpendicular to the plane of the central benzene ring in **1**, is 3.940(1) Å. Figure 3 is an ORTEP representation of the asymmetric unit.

Single crystals of **8**, as the MeOH solvate**,** were grown by diffusion of MeOH into a 1:1 MeCN solution of AgOTs and ligand **4**. The structure of **8**·MeOH (Figure 4) also reveals the formation of an infinite two-dimensional array consisting of cationic Ag(**4**) layers reinforced by a coordinating *p*-toluenesulfonate anion as well as the hexoxy substituents on the ligand. The structure does adopt a bilayer arrangement as opposed to interdigitated monolayers. The interlayer distance in **8,** defined as the perpendicular distance between Ag^{I} ions, is 18.930(1) Å (cf. 11.230(1) Å in **5**·$(benzene)_{0.5}$). The alkyl group functionality of the ligand is pointing directly into the interlayer region, and the OTs anion is imbedded in this hydrophobic domain. On examination of a single layer (Figure 5), the geometry at Ag^{I} is a distorted octahedron. The coordination sphere is comprised of four equatorial thioether donors, with a single long Ag−S interaction (Ag−S1 = 2.470(4) Å, Ag−S1a = 3.230(5) Å, Ag−S2 = 2.532(4) Å, Ag−S2a = 2.928(5) Å), and a sulfonate oxygen (Ag−O5 = 2.596(5) Å) and weakly bound methanol (Ag−O = 2.814(5) Å) in the equatorial position. Each sulfur atom of **4** employs both lone pairs to interact with two different silver ions. The lamellae are not perfectly flat as the distorted geometry at Ag necessitates a slight ruffling of the layers. In **8**, ligand **4** is observed solely in the anti conformation, with respect to the orientation of the sulfur donors in the slightly puckered pentagonal rings. The alkane chain is oriented at an angle of 48.1(1)° to the mean plane of the Ag ions. The toluenesulfonate anion is coordinated to the silver ions and orients itself at an angle of 63.1(1)° to the mean lamellar plane. The ligand−ligand separation, measured perpendicular to the plane of the central benzene ring, is 4.222(4) Å. Figure 6 is an ORTEP representation of **8**·MeOH.

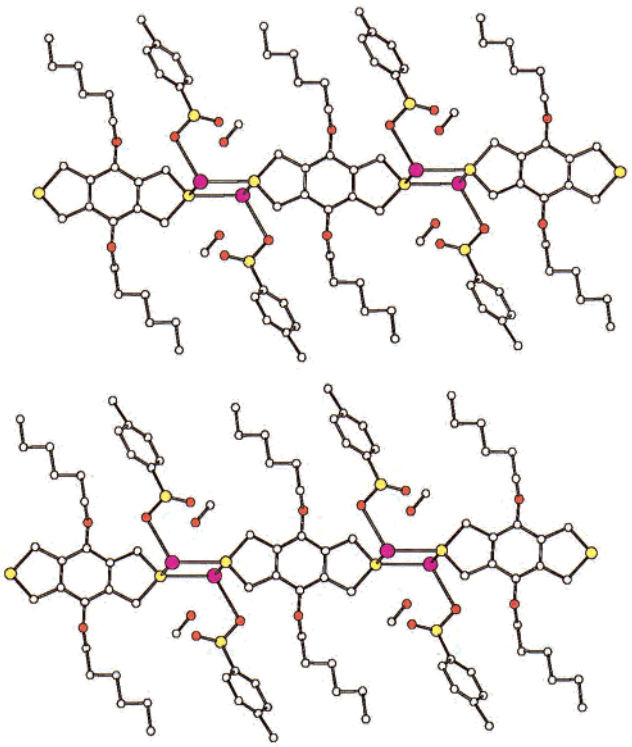

Figure 4. Single-crystal X-ray structure of **8** showing the two-dimensional motif: Ag, large spheres; S, medium spheres; O, small dark spheres; C, small white spheres. Note that the alkyl chains are directed into the interlayer region and MeOH is adjacent to the SO_3 group.

For compound **9**, $AgPF_6$ was added to a MeCN solution of **1** in a 1:1 molar ratio. A diffusion of isopropyl ether was stored in the dark under N_2 at 5 °C. This gave colorless, needlelike crystals of $[Ag(\mathbf{1})(MeCN)_2]PF_6$, suitable for an X-ray analysis. Compound **9** no longer forms layered networks but, rather, parallel sheets of one-dimensional coordination polymers. Viewed down the *b*-axis, the structure of **9** (Figure 7) resembles the other frameworks with repeating $[Ag(\mathbf{1})(MeCN)_2]^{+}$ units separated by PF_6^{-} ions. However, a view perpendicular to the *b*-axis (Figure 8) clearly shows that a layered structure no longer

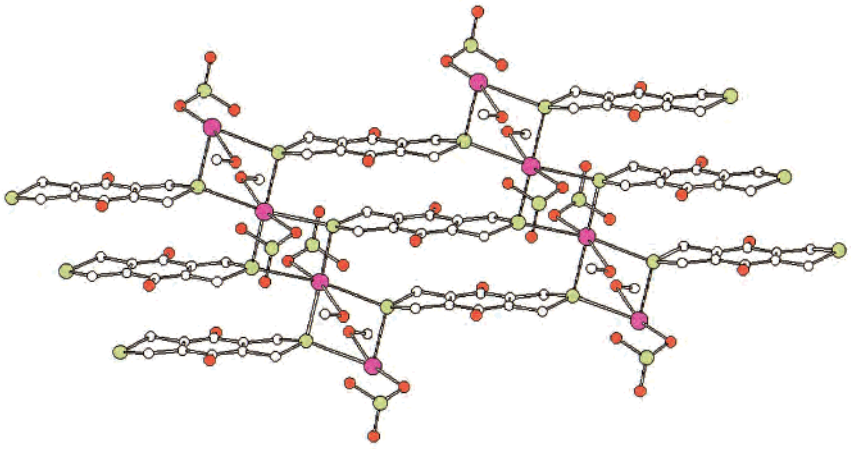

Figure 5. View of a single layer of **8** showing the distorted square pyramidal geometry at Ag and the bridging coordination mode of the ligand. Hexyl and toluene groups are omitted for clarity.

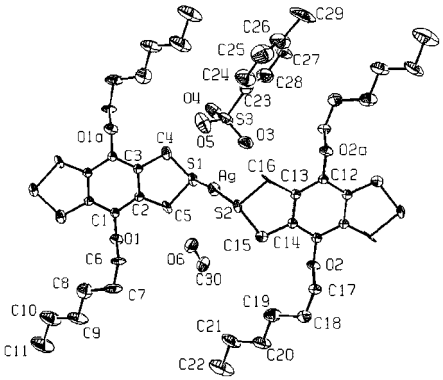

Figure 6. ORTEP plot of the asymmetric unit of **8** showing the numbering scheme. Thermal ellipsoids of 50% probability are represented.

exists. The asymmetric unit consists of one half-occupied Ag site, half a molecule of **1**, one-half of a PF_6 ion disordered over two sites, and 1 equiv of MeCN in which the N is full occupancy and the two carbon atoms are disordered over two sites. The disorder concerning the PF_6 ion and the MeCN molecule may be described as the MeCN ligand pivoting on the coordinated N atom to switch positions 50% of the time. The PF_6 ion alternates positions with the MeCN ligand resulting in the occupancies stated above. The geometry at the metal center is a distorted tetrahedron comprised of two thioether donors and two acetonitrile N atoms (Ag−S = 2.563(1) Å, Ag−N = 2.340-(5) Å). Each molecule of **1** is ligated to two silver ions to form a zigzag 1-D array. Importantly, the additional Ag−S interaction(s) involving a third ligand as in **5** (or a fourth ligand as in **8**) is not observed. In **5** and **8**, these interactions are responsible for transforming 1-D ribbons into 2-D layers. The shortest *inter*chain Ag−S distance in **9** is 3.525(3) Å, a value beyond bonding distance. Adjacent molecules of **1** are parallel and are at a distance of 3.906(1) Å. In **9**, ligand **1** is observed solely in the anti conformation, with respect to the orientation of the sulfur donors in the pentagonal rings. The interchain distance in **9**, analogous to the interlayer distance in the other complexes, is 10.455(1) Å. Figure 9 is an ORTEP representation of the asymmetric unit of **9**.

Powder X-ray Diffraction of AgOTs Complexes, 5−8. Samples of complexes **5**−**8** as precipitated powders were studied by powder X-ray diffraction (PXRD) as shown in Figure 10 and compared to simulations of the PXRD from the single-crystal data of **5**·(benzene)$_{0.5}$ and **8**·MeOH. The *d*-spacings, corresponding to the 2θ value of the dominant peak in the PXRD patterns of **5**−**8,** are 9.21, 12.22, 16.07, and 19.28 (±0.05) Å, respectively. The PXRD pattern observed for compound **5**, in Figure 10a, differs from the crystal structure by the fact that benzene is included in the interlayer, resulting in a smaller *d*-spacing observed for the dry compound as expected (11.230-(1) compared to 9.21(5) Å). However, desolvated single-crystal samples of **5**·(benzene)$_{0.5}$ show the same PXRD as Figure 10a. A powder X-ray diffraction pattern, simulated from the single-crystal data of **8**·MeOH, correlated well with that shown in Figure 1d. The principal Bragg peak for **8** corresponds to a long axis of 19.28(5) Å, and the crystallographically observed *c*-axis is 19.308(9) Å. These values would not be expected to correspond exactly because of the presence of interlamellar MeOH in the single-crystal structure, which would increase the observed axis length, and the fact the single-crystal data was obtained at −100 °C, which would cause a decrease in the observed value. These factors offset to give values that match within experimental error. The implication of these data is that the alkyl group of the ligands is directed into the interlayer region and is forcing the lamellae apart. The length of an all-trans polyalkane chain increases linearly by approximately 2.5 Å for every two methylene units appended. The interlayer distances observed for the alkoxy-functionalized complexes are beyond the range attainable for a single chain and are consistent with the formation of bilayer structures rather than interdigitated monolayers. This observation is also consistent with the crystal structure of **8**·MeOH. A noteworthy observation is the sequential decrease in the resolution of the PXRD patterns in going from compound **5** to compound **8**. This is not a surprising result because in **5**, the groups that determine the character of the interlayer region are rigid toluene moieties. In **8**, the nature of the interlayer is defined by a bilayer of flexible hexoxy groups.[13]

Upon comparison of the similar chemical analysis and PXRD of compounds **5** and **8**, the structures of **6** and **7** can be inferred to be layered networks in which the organic functionality protrudes, to a lesser degree, into the interlayer region. The two-dimensional structure of compounds **6** and **7** is further born out by the thermal analysis as discussed in the next section. Significantly, despite the nature of the pendant R-group on the

(13) The AgOTs complex of the bis(octoxy) derivative of the ligand was also synthesized, but a complete structural characterization of this complex was difficult because, despite technically being an inorganic salt, the complex was an oil. This observation, however, is in keeping with the existing trend in complexes **5**−**8** (i.e., that the networks lose their saltlike properties as the layers become sheathed in an organic coat).

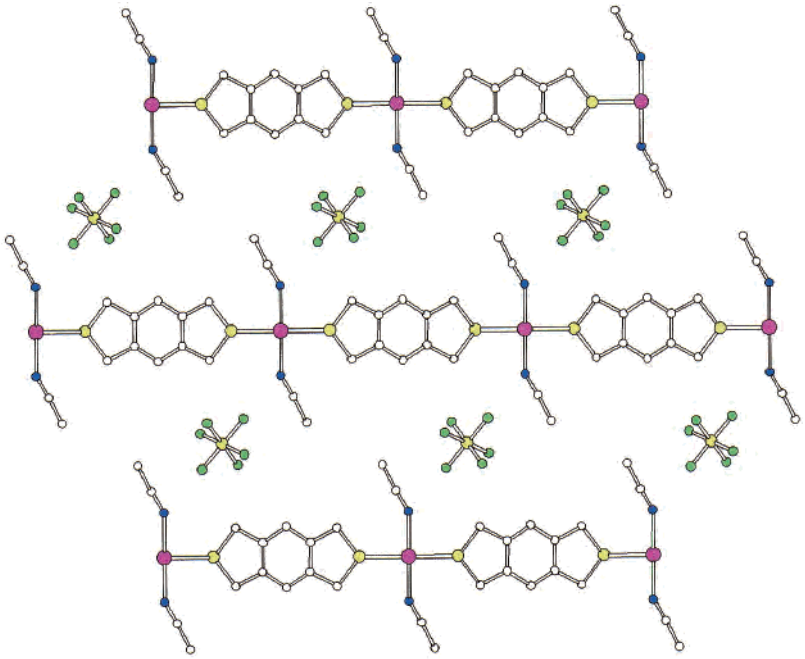

Figure 7. Single-crystal X-ray structure of **9** viewed down the *b*-axis: Ag, large spheres; S, medium spheres; N, small dark spheres; C, small white spheres. For clarity, only one set of positions of the disordered MeCN and PF_6 are shown.

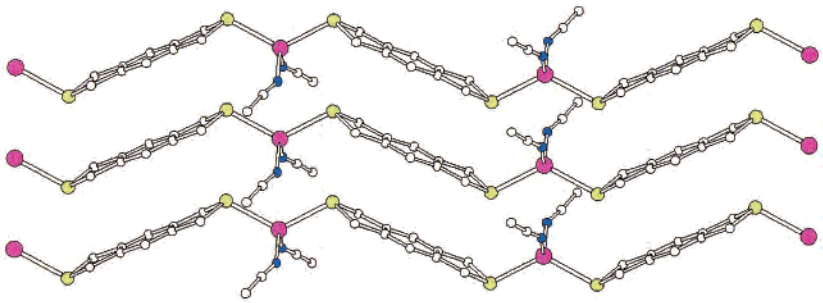

Figure 8. Single-crystal X-ray structure of **9** viewed perpendicular to the *b*-axis, showing the one-dimensional structure and Ag atoms ligated to only two S atoms.

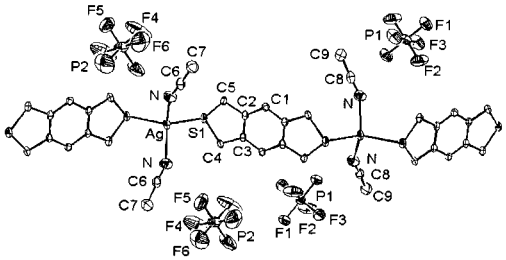

Figure 9. ORTEP plot of the asymmetric unit of **9** showing the numbering scheme. Thermal ellipsoids of 50% probability are represented.

central benzene core changing from a hydrogen atom to a hexoxy group, layered structures are observed for each of the complexes **5**−**8**. We are aware of only two other studies directed at forming systematically tunable layered coordination networks. In neither of these works do the authors synthesize a family of sequentially modified ligands.[14]

Thermal Stability and Cooperative Bonding Effects. Differential scanning calorimetry/thermogravimetric analysis (DSC/TGA) analyses of complexes **5**−**8** reveal thermal stabilities of 166, 212, 171, and 166 °C, respectively. The range of values is likely an indication of the efficiency of the interlayer packing and, hence, the stability of the layer, as compounds **5** and **8** include solvent. Monodentate thioethers are generally regarded as very poor ligands for transition metals. In fact, homoleptic transition metal complexes of Me_2S have been referred to as "virtually impossible to prepare".[5] Thus, it is interesting to note that each of the ligands **1**−**4**, which can be pictured as two molecules of Me_2S linked by an aromatic spacer in a nonchelating fashion, forms complexes stable to over 160 °C with the typically air and light sensitive silver(I) ion. This stability stems from the regimented coordination environment about the Ag^+ center as enforced by the layered structure. In essence, it is not possible to break bonds to any one metal center; multiple Ag−S interactions must be overcome simultaneously. In the case of compound **9**, reproducible thermal analysis data were exceedingly difficult to obtain as the crystals decomposed rapidly during sample preparation at ambient conditions. This behavior is readily explained by the lower dimensionality of the network. Although the Ag center in **9** is four-coordinate, two of the ligands are labile MeCN molecules and distance to the nearest interribbon S atom is 3.525(3) Å. This nonbonding distance restricts the framework to one dimension and results in its highly compromised stability. These complexes are an

(14) (a) Kawata, S.; Kitagawa, S.; Kumagai, H.; Ishiyama, T.; Honda, K.; Tobita, H.; Adachi, K.; Katada, M. *Chem. Mater.* **1998**, *10*, 3902. (b) Kawata, S.; Kitagawa, S.; Kumagai, H.; Kudo, C.; Kamesaki, H.; Ishiyama, T.; Suzuki, R.; Kondo, M.; Katada, M. *Inorg. Chem.* **1996,** *35*, 4449.

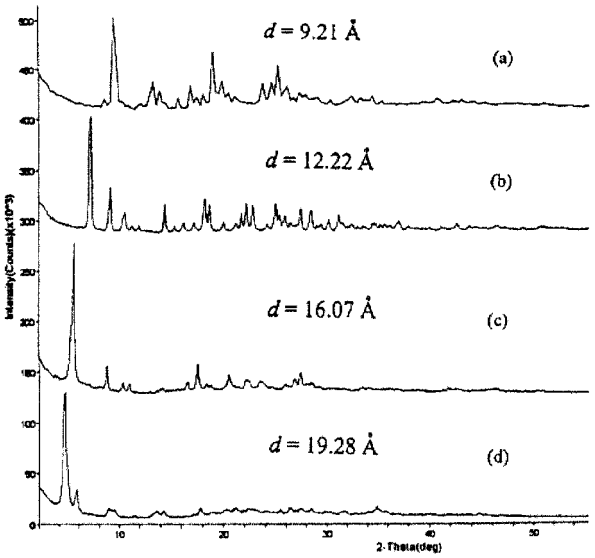

Figure 10. The PXRD patterns (Mo Kα radiation) obtained for the AgOTs complexes of the derivatized ligands, (a) **5**, (b) **6**, (c) **7**, (d) **8**, showing increasing *d*-spacings (and loss of resolution) with increasing alkyl chain length on the ligand.

excellent example of enhanced stability via cooperative bonding effects, so frequently discussed for hydrogen-bonding interactions,[15] in an extended network.[16] Conversely, compound **9** serves to illustrate, via the loss of an Ag−S interaction, the structural factors which can determine a critical stabilization threshold. It should be noted that robust thioether complexes of Ag^I are typically stabilized by either macrocyclic chelate effects,[17] involvement of the formation of an infinite *multi*dimensional framework,[4] or, in some cases, both effects.[4g,h,j]

Conclusions

The family of Ag coordination networks presented herein demonstrates that despite the use of supposedly weaker metal−ligand interactions, very stable coordination networks can be generated once cooperative binding effects come into play. Stable layered frameworks are formed even when the ligand core is derivatized with two hexoxy groups. However, altering the counteranion causes a shift from a two-dimensional to a one-dimensional framework, reduces cooperative bonding effects, and consequently greatly compromises the stability of the structure.

Acknowledgment. This research was funded by an award from Research Corporation and the National Sciences and Engineering Research Council of Canada.

Supporting Information Available: X-ray crystallographic files for compounds **5**, **8**, and **9**, in CIF format, are available. This material is available free of charge via the Internet at http://pubs.acs.org.

IC0103749

(15) Jeffrey, G. A.; Sainger, W. *Hydrogen Bonding in Biological Structures*; Springer-Verlag: Berlin, 1991; p 569.

(16) To further verify this effect, a control experiment was performed in which the monothia derivative of **1** was synthesized and complexation with silver(I) was studied. Without the enhanced stability provided by the network formation, none of the AgOTs, $AgPF_6$, or $AgBF_4$ salts formed stable complexes. In fact, the PF_6^- and BF_4^- salts underwent immediate photolysis and decomposition.

(17) (a) Casabo, J.; Flor, T.; Hill, M. N. S.; Jenkins, H. A.; Lockhart, J. C.; Loeb, S. J.; Romero, I.; Teixidor, F. *Inorg. Chem.* **1995**, *34*, 5410. (b) Alberto, R.; Nef, W.; Smith, A.; Kaden, T. A.; Neuburger, M.; Zehnder, M.; Frey, A.; Abram, U.; Schubiger, P. A. *Inorg. Chem.* **1996**, *35*, 3420. (c) De Groot, B.; Loeb, S. J.; Shimizu, G. K. H. *Inorg. Chem.* **1994**, *33*, 2663. (d) Blower, P. J.; Clarkson, J. A.; Rawle, S. C.; Hartman, J. R.; Wolf, R. E., Jr.; Yagbasan, R.; Bott, S. G.; Cooper, S. R. *Inorg. Chem.* **1989**, *28*, 4040.